NANO LETTERS

Letter

pubs.acs.org/NanoLett

Observation of a Transient Decrease in Terahertz Conductivity of Single-Layer Graphene Induced by Ultrafast Optical Excitation

Giriraj Jnawali,[†] Yi Rao,[‡] Hugen Yan,[§] and Tony F. Heinz*[,†]

[†]Departments of Physics and Electrical Engineering and [‡]Department of Chemistry, Columbia University, New York, New York 10027, United States

[§]IBM T. J. Watson Research Center, P.O. Box 218, Yorktown Heights, New York 10598, United States

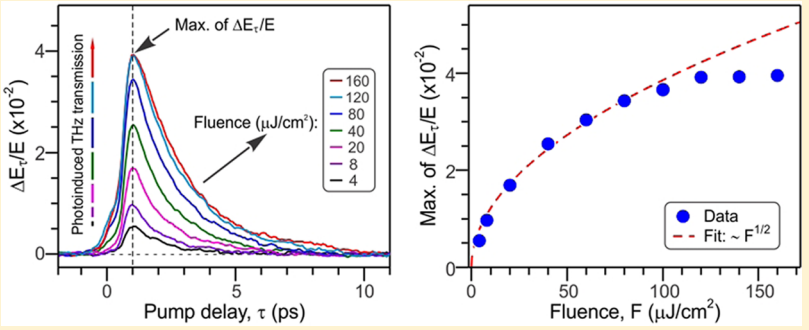

ABSTRACT: We have measured the terahertz frequency-dependent sheet conductivity and its transient response following femtosecond optical excitation for single-layer graphene samples grown by chemical vapor deposition. The conductivity of the unexcited graphene sheet, which was spontaneously doped, showed a strong free-carrier response. The THz conductivity matched a Drude model over the available THz spectral range and yielded an average carrier scattering time of 70 fs. Upon photoexcitation, we observed a transient *decrease* in graphene conductivity. The THz frequency-dependence of the graphene photoresponse differs from that of the unexcited material but remains compatible with a Drude form. We show that the negative photoconductive response arises from an increase in the carrier scattering rate, with a minor offsetting increase in the Drude weight. This behavior, which differs in sign from that reported previously for epitaxial graphene, is expected for samples with relatively high mobilities and doping levels. The photoinduced conductivity transient has a picosecond lifetime and is associated with nonequilibrium excitation conditions in the graphene.

KEYWORDS: *Graphene, terahertz conductivity, transient photoconductance, carrier scattering, THz time-domain spectroscopy*

Single-layer graphene is a gapless two-dimensional material with linear electronic band dispersion for the electron and hole bands near the corners of the Brillouin zone.[1,2] The charge carriers in this system behave like massless Dirac fermions and have high Fermi velocity and mobility.[1−5] Moreover, graphene shows attractive photonic properties,[6,7] driven by strong absorption of light over a very broad spectral range,[8−11] which can be further tuned by changing the Fermi energy using an external gate field.[12,13] With its exceptional electronic and optical properties, graphene shows promise in the application of high-speed optoelectronic devices.[6,7,14−19] The implementation of such devices requires fundamental understanding of the material's optical conductivity and its dynamical response over a wide range of frequencies from THz to UV.

The optical response of graphene from visible to infrared frequencies has been extensively investigated. It is known to be dominated by interband absorption, with an optical sheet conductivity of $\sigma_0 = \pi G_0/4$, where $G_0 = 2e^2/h$ is the quantum of conductance,[8,9,20,21] In the far-IR and THz spectral region, the intraband response in graphene becomes pronounced, leading to the possibility of strong extinction in single-layer graphene[11,22−27] as well as of plasmon excitation through appropriate coupling.[17,28−30] Understanding the dynamics of this optical response to photoexcitation is a topic of both fundamental interest and of critical importance for the development of high-performance optoelectronic devices. While many studies have been performed probing evolution of the graphene optical response following ultrafast carrier excitation,[31−37] the transient response in the THz spectral regime has been investigated to a more limited extent.[38−40] This transient THz response is of particular interest since it directly interrogates the dynamics of the free carriers, without the complication of interband transitions. The response of carriers under nonequilibrium conditions is of particular importance in view of recent advances in the generation of photocurrent[41−49] and operation of photodetectors in graphene.[50,51]

In this paper, we report measurement of the frequency-dependent sheet conductivity $\sigma(\omega)$ of graphene grown by

Received: October 29, 2012
Revised: January 15, 2013
Published: January 18, 2013

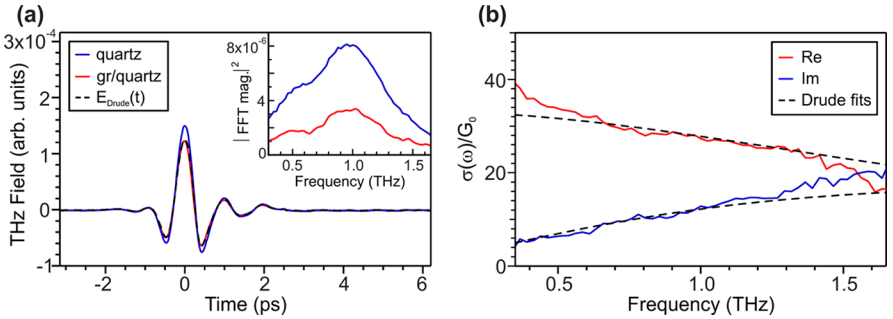

Figure 1. Response of the unpumped graphene layer at THz frequencies. (a) Measured THz electric-field waveforms transmitted through the bare quartz substrate (blue) and the substrate with a graphene overlayer (red). The inset shows the squared magnitudes of Fourier transforms of the corresponding time-domain signals. (b) Complex sheet conductivity of the graphene layer, extracted from the relative transmission. The conductivity spectra are normalized by the quantum of conductance $G_0 = 2e^2/h$. A fit of the complex conductivity to a Drude model (dashed lines) is shown. The Drude response has been converted into a time-domain waveform and is shown in part a as a dashed line for comparison with the measured THz waveform.

chemical vapor deposition (CVD) following ultrafast optical excitation. Using THz time-domain spectroscopy in conjunction with a femtosecond optical pump pulse, we record the transient photoconductive response of the graphene. The initial THz spectrum prior to excitation is found to be compatible with a Drude response of carriers exhibiting a scattering time of ~70 fs and substantial carrier doping. This result is compatible with properties expected for the relatively high mobility graphene samples, grown by chemical vapor deposition (CVD), that were employed in our study. Upon photoexcitation, we observe an ultrafast decrease in conductivity, which persists for a few picoseconds. This behavior stands in sharp contrast to previous reports[38−40] of the response of epitaxial graphene layers to optical excitation where an increased conductivity was induced by ultrafast optical excitation. Also unlike the earlier studies, our measurements are able to follow the temporal evolution of the THz conductivity spectrum under nonequilibrium conditions. We find that the transient conductivity still exhibits a Drude response after photoexcitation, but with a clear increase in scattering rate. The negative transient photoconductivity can thus be attributed to decreased carrier mobility, with little change in the Drude weight, in the nonequilibrium regime. The role of carrier mobility and concentration in controlling both the magnitude and the sign of the ultrafast photoreponse of graphene is discussed on the basis of our findings.

The graphene samples examined in this study were prepared using CVD. The single-layer graphene was grown on Cu foil at temperatures up to 1000 °C using a mixture of methane and hydrogen.[52] The graphene layers on Cu were then transferred to quartz substrates by means of a poly(methyl methacrylate) (PMMA) coating and etching of the copper foil. Raman scattering measurements confirmed the single layer thickness of the samples and their low defect density.[11]

Our measurements made use of optical excitation of the graphene by a femtosecond pulse and probing of the THz response using a time-domain spectroscopy approach. The laser excitation for both optical pumping and THz probing was a regenerative Ti:sapphire amplifier system, which produced 2 mJ, 120 fs pulses at repetition rate of 1 kHz and a central wavelength of 800 nm. THz pulses were generated from the femtosecond laser pulses by means of optical rectification in a 1 mm thick ZnTe(110) crystal.[53] The emitted THz radiation was collimated and focused by a pair of off-axis parabolic mirrors onto the graphene sample. The size of the THz beam on the graphene sample was about 2 mm. After passing through the sample, the diverging THz radiation was collimated and focused by another pair of off-axis parabolic mirrors onto another 1 mm thick ZnTe(110) crystal. The THz field was detected by free-space electro-optic sampling (EOS).[53−55] The sampling beam was scanned in time using an optical delay stage. The signal was collected with a lock-in amplifier phase-locked to an optical chopper that modulated either the THz generation arm or the pump beam at a frequency of 500 Hz. The former case permitted measurement of the THz waveform, while the latter yielded the differential change of the THz waveform induced by optical excitation of the sample.

For optical excitation, the pump irradiated the sample at an angle of 5° from surface normal. To ensure probing of an homogeneously photoexcited region, a pump beam diameter of 5 mm was used, significantly larger than the 2 mm spot size of the normally incident THz beam. A second optical delay stage in the path of the pump beam allowed us to vary the time delay of the THz probe pulse with respect to the optical excitation pulse. The entire THz beam path was enclosed and purged with dry nitrogen to avoid water vapor absorption. All of the measurements were performed at room temperature and under ambient conditions.

Characterization of the THz conductivity of the unpumped graphene sample was obtained from THz time-domain spectroscopy measurements performed in a transmission configuration. We recorded the time-dependent electric field of the THz wave transmitted through the graphene monolayer on the quartz substrate, $E(t)$, and, as a reference, through the bare quartz substrate, $E_0(t)$. Fourier transformation then yields the corresponding (complex) frequency-domain fields, $E(\omega)$ and $E_0(\omega)$. Figure 1a shows the THz time-domain transmission scans with and without the graphene sample, as well as the corresponding power spectra, that is, $|E(\omega)|^2$ and $|E_0(\omega)|^2$. A significant attenuation of THz transmission can be observed immediately, arising from the strong response of charge carriers in the graphene.

Applying the standard thin-film approximation,[56,57] we can extract the frequency-dependent complex sheet conductivity $\sigma(\omega)$ of the graphene monolayer from the measured transmission spectra by application of the relation

$$\frac{E(\omega)}{E_0(\omega)} = \frac{n+1}{n+1+Z_0\sigma(\omega)} \quad (1)$$

dx.doi.org/10.1021/nl303988q | Nano Lett. 2013, 13, 524−530

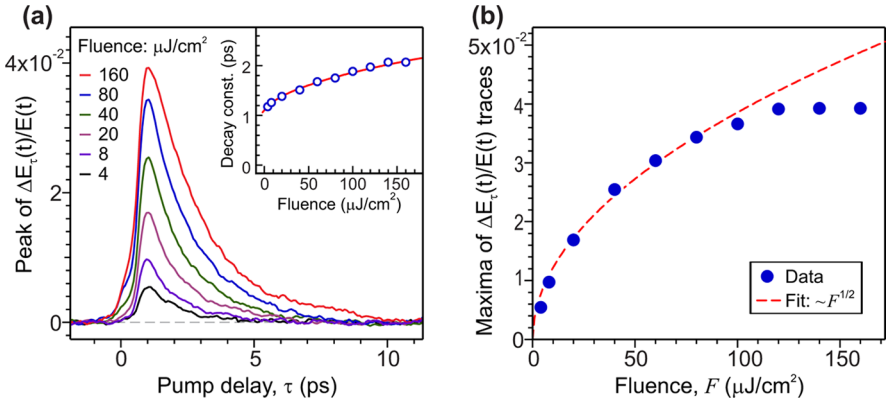

Figure 2. Transient THz transmission response of photoexcited graphene layer: (a) temporal evolution of the change in the maxima of the transmitted THz waveforms normalized by the THz probe field, i.e., $\Delta E_\tau(t)/E(t)$, for different applied fluences of optical pump pulse. The inset shows the decay times of the pump-induced THz response, extracted from part a by fitting with single exponential function. (b) Maxima of the time traces of $\Delta E_\tau(t)/E(t)$ from part a as a function of applied fluence, which saturates at higher fluences. The dashed line varies as the square root of the fluence, as a guide to the eye.

Here $Z_0 = 377\ \Omega$ is the impedance of free space, and n is the refractive index of the substrate. We treat the THz refractive index of the fused quartz substrate as dispersion-free and having a value of $n = 1.96$.[58,59]

Figure 1b shows the resulting complex sheet conductivity of the graphene layer in the THz spectral range. The (real part of the) sheet conductivity of the graphene sample in the DC limit is nearly $30G_0$. This large conductivity is expected because of the high carrier concentration arising from the sample growth and transfer process, combined with the relatively high carrier mobility. The results of the THz time-domain measurement were found to be in good agreement with the absorption spectra obtained by conventional frequency-domain Fourier-transform infrared spectroscopy.[11] The decreasing real part of the conductivity observed for increasing THz frequency indicates that the scattering time in the graphene sample is sufficiently long so that the carriers can respond to the oscillatory character of the THz field. This behavior differs from that reported in several other studies of CVD-grown graphene,[23,24,27,38,39,60] where the scattering rate was evidently too high to observe any frequency dependence of the conductivity over the accessible THz spectral range.

To understand the transport properties more fully, we compare the experimental conductivity with the predictions of a Drude response for charge carriers in graphene:[61−65]

$$\sigma(\omega) = \frac{D}{\pi}\frac{1}{(\Gamma - i\omega)} \tag{2}$$

Here Γ is the average scattering rate for momentum changing collisions of charge carriers. The Drude weight D characterizes the magnitude of the response. In the limit of a degenerate electron gas relevant in our measurements (thermal excitation energy $k_BT \ll E_F$, the Fermi level for the carriers), the Drude weight can be written as $D = (v_F e^2/\hbar)(\pi|N|)^{1/2}$, with v_F denoting the Fermi velocity and N the sheet density of carriers.

As shown in Figure 1b, the Drude model fits the experimental values of the complex conductivity well within the spectral range of 0.3−1.6 THz where we have sufficient power for reliable measurements. The best fit to the experimental graphene conductivity yields a Drude weight of $D = 6.96 \times 10^3 G_0$ cm^{-1} and a carrier scattering rate of $\Gamma = 75.8$ cm^{-1}. Applying the relation between the Drude weight and the charge density, we infer $N = 4.60 \times 10^{12}$ cm^{-2}. From the carrier density, we can estimate the Fermi energy as $E_F = -275$ meV using the expression for the Fermi energy of the Dirac Fermions, $E_F = (N\hbar^2 v_F^2 \pi/e^2)^{1/2}$, with a Fermi velocity[2] of $v_F = 1.1 \times 10^6$ m/s. (The negative value of the Fermi energy corresponds to the known hole doping for these transferred, CVD-grown graphene films.) The estimated Fermi energy is consistent with the complementary Fourier transform infrared spectroscopy (FTIR) measurements.[11] Using the carrier density, we find a carrier mobility of the graphene sample of approximately 3000 cm^2/V·s.

We now present results on the pump-induced change in the THz conductivity and its dynamics. This response was examined by recording the transmitted THz electric field at different fixed delay times between the pump pulse and THz probe pulse. By placing the chopper in the pump beam, we could directly record the differential electric field for the transmitted THz beam, that is, $\Delta E_\tau(t) = E_\tau(t) - E(t)$, where $E(t)$ is the transmitted THz waveform through the unpumped graphene and $E_\tau(t)$ is the THz waveform for the pumped sample recorded for delay time τ. The differential waveforms show a substantial phase shift (peak-to-peak shift > 120 fs) compared to the probe waveform $E(t)$. Rather than a simple change in the amplitude of the transmitted field with pump excitation, the change in THz waveform indicates the role of the finite carrier scattering time in our graphene samples.

To investigate the relaxation dynamics of the graphene sample, we record the peak of the pump-induced differential signal $\Delta E_\tau(t)$ as a function of probe delay τ. Figure 2a presents the corresponding data for the change in the maxima of THz waveforms $\Delta E_\tau(t)$ normalized by the peak of the probe field $E(t)$. For all pump fluences investigated, the THz transmission increases rapidly after photoexcitation (on the time scale of 1 ps) and then recovers to the original value on the time scale of a few picoseconds. We have repeated such measurements on our several samples and found consistent results of pump-induced change and relaxation dynamics, suggesting no sensitive dependence on possible contaminants or defects in the graphene. The fluence dependence of the dynamics will be revisited after the discussion of the origin for the photoinduced change in the THz conductivity.

The increased THz transparency of the graphene sample after photoexcitation corresponds to a photoinduced *decrease* in the THz conductivity. This result is unexpected in the context

dx.doi.org/10.1021/nl303988q | Nano Lett. 2013, 13, 524−530

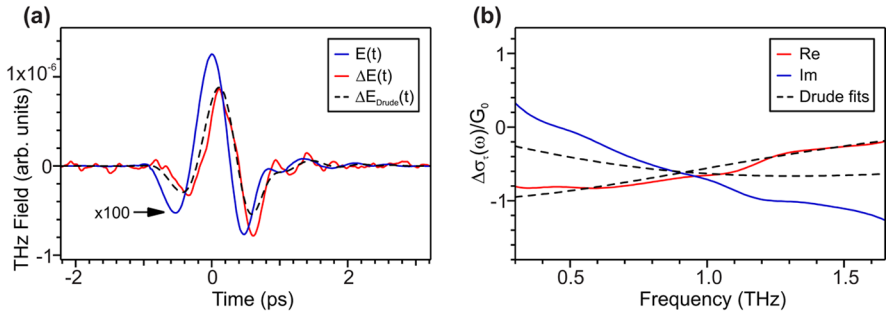

Figure 3. Photoinduced change in the THz transmission through graphene and inferred change in the graphene conductivity. (a) The THz electric field $E(t)$ transmitted through the graphene sample (blue line) together with the pump-induced waveform, $\Delta E(t)$ (red line) at a fixed pump−probe delay of $\tau = 2.5$ ps. (b) The photoinduced change in the complex THz conductivity $\Delta\sigma_\tau(\omega)$ of the graphene layer extracted from the pump-induced THz response in part a. The dashed lines are fits based on a Drude model for the response of graphene both before and after photoexcitation, as described in the text. The Drude fits are converted into a predicted time-domain waveform $\Delta E_{\mathrm{Drude}}(t)$, which, as shown in part a with dashed black line, agrees well with the experimental data for the pump-induced THz response.

of photoexcitation of a semiconductor. In a semiconductor, photoexcitation normally generates free carriers and increases conductivity, that is, produces a positive photoconductivity.

The physical origin of the observed effect can be understood by considering the Drude conductivity of graphene in the low-frequency limit. The THz behavior, at least for lower frequencies, will be qualitatively similar. In the DC limit, we have a real conductivity of $\sigma = D/\pi\Gamma$. Thus, photoinduced changes in both the Drude weight D and scattering rate Γ can affect the conductivity. Under excitation, the D may increase through a rise in the carrier concentration, while Γ may increase through a rise in the effective temperature of the system. Depending on the initial Drude weight, the scattering rate of the unpumped graphene, and the pump fluence, the ratio of D/Γ and, hence, the conductivity can either increase or decrease after photoexcitation. For a system that behaves like a conventional semiconductor, one would expect the main effect to be an increase in the carrier density, leading to enhanced conductivity through a larger increase in D than in Γ. On the other hand, when the main effect of photoexcitation is an increase in the Drude scattering rate Γ, then a photoinduced decrease in conductivity is expected. This latter case would apply to photoexcitation of a conventional metal, where the excitation would not produce a large sustained change in carrier concentration but could increase the scattering rate appreciably. Graphene can exhibit either type of behavior for the transient response, depending on the detailed conditions. When the initial doping level and scattering time are both relatively high, we would anticipate the main effect to be that of change in the scattering rate, rather than the change in the Drude weight, that is, a response more like that of a metal. This is the case observed in these measurements.

For a more quantitative analysis of the THz response of graphene after photoexcitation, we extract the frequency-dependent transient photoconductivity of the graphene sample for a given delay time τ of the THz probe with respect to the pump beam. Within a quasi-static picture of the graphene response, we find the induced change in THz conductivity $\Delta\sigma_\tau(\omega)$ from the modification of the transmitted electric field induced by photoexcitation, $\Delta E_\tau(t)$, compared to the field transmitted through the unexcited graphene layer, $E(t)$. We do so using the relation[57,66] for a small differential change in eq 1:

$$\Delta\sigma_\tau(\omega) \approx -\frac{n+1}{Z_0}\frac{\Delta E_\tau(\omega)}{E(\omega)} \qquad (3)$$

Here $\Delta\sigma_\tau(\omega)$ and $E(\omega)$ are the Fourier transforms of the corresponding time-domain signals. This expression is valid when the perturbation to the THz response is slight and absorption from the substrate is relatively weak (<20%).[67] Both conditions are fulfilled in our measurements.

Figure 3a shows the induced response in graphene for an applied pump fluence of 20 μJ/cm^2 and a probe delay of $\tau = 2.5$ ps. This delay time was chosen to eliminate the effect of the initial transient response on the photoinduced THz waveform. The experimental results are shown both in the time domain (a) and in the frequency domain (b) after Fourier transformation. As expected from the enhanced transparency after pumping, the real part of $\Delta\sigma_\tau(\omega)$ is seen to be negative over the accessible THz frequency range; that is, we observe a negative transient photoconductivity.

We model the transient response assuming that both the initial (unpumped) response of the graphene layer and its response after photoexcitation can be described by a Drude form, but each with its own Drude weight and scattering rate. We denote the initial graphene Drude weight by D and the Drude weight for at a time delay τ after the optical excitation pulse by D_τ, with scattering rates Γ and Γ_τ designated similarly. We then fit the pump-induced differential change in the THz conductivity $\Delta\sigma_\tau(\omega)$ with D_τ and Γ_τ as adjustable parameters, but D and Γ fixed by the THz measurements on the unperturbed graphene. The dashed line in Figure 3b shows the best-fit result in the frequency domain. Despite some deviations in the imaginary part, the model agrees fairly well within this simple Drude analysis. The discrepancy may be caused by the limited terahertz beam intensity for frequency regimes above 1.5 THz. The fit for the differential change in the THz waveform is also presented directly in the time domain in Figure 3a. Again good overall agreement is seen, given the simplicity of the model.

The parameters for the fit of the transient conductivity are $D_\tau = 6.98 \times 10^3\ G_0$ cm^{-1} and $\Gamma_\tau = 78.2$ cm^{-1}. These values correspond to an increase of Drude weight of $\Delta D = 20\ G_0$ cm^{-1} and an increase of scattering rate of $\Delta\Gamma = 2.4$ cm^{-1}. Although the fractional changes of both parameters D and Γ induced by the optical pumping are modest (0.3% and 3.1%, respectively), we note that the dominant change is an increase in the carrier scattering rate, rather than an increase in the Drude weight. This explains the observed negative THz photoconductivity response.

dx.doi.org/10.1021/nl303988q | Nano Lett. 2013, 13, 524−530

We now consider briefly the physical origin of the pump-induced changes in the Drude weight and scattering time for graphene deduced from the measurements. On the time scale of these measurements, previous investigations indicate that the femtosecond pump excitation leads to electrons and holes in the graphene that are thermalized with a common chemical potential.[68] Certain strongly coupled optical phonons are also described by this temperature, with cooling of this subsystem by emission of other phonons occurring on the time scale of a few picoseconds.[68] Within this picture, we can estimate the increase in the Drude weight using a relation for the temperature and density dependent Drude weight of carriers in graphene by Gusynin et al.[69] From studies of time-resolved Raman spectroscopy of graphite[70] and ultrafast photoluminescence from graphene,[68] we estimate the temperature of the electrons in graphene for a typical applied fluence of 20 μJ/cm^2 to be less than 500 K at the 2.5 ps pump−probe delay. With an initial Fermi level of −275 meV, the increase in the Drude weight calculated using the results of ref 69 is less than 0.2%. This is in good agreement with the very slight change in the Drude weight observed experimentally.

With respect to the scattering rate, earlier experiments[71] have established that the carrier scattering for graphene samples on SiO_2 surfaces arises largely from impurity scattering, which is essentially independent of temperature over the relevant range. Above room temperature, however, scattering by surface polar phonons in the SiO_2 substrate plays an important role.[71] The increased electronic temperature of the carriers in graphene following pump excitation should then lead to enhanced scattering rate through this channel, which could naturally explain the observed 3% increase in Γ following excitation of the graphene. For higher temperatures, the role of optical phonon scattering could also be important.

The THz response observed for photoexcited graphene in this investigation differs from that seen in previous studies,[20,25,40] in which a spectrally flat response of THz transmission was observed for both static and photoinduced measurements. In addition, the photoinduced response reported earlier was a decrease in the THz transmission, corresponding to an increased conductivity of graphene. The lack of variation with THz frequency is attributable to higher scattering rates in graphene samples studied previously than in the relatively high mobility sample examined in this study. The difference in the sign of the photoinduced conductivity may reflect a number of factors. For the case of high scattering rates that were relevant in the previous reports in the literature, the intrinsic properties of graphene are expected to be dominated by impurity scattering processes. This scattering channel exhibits little temperature dependence and, consequently, will not be significantly altered by optical pump excitation. A photoinduced increase in the Drude weight is then likely to dominate the THz response, particularly if the initial doping of the sample is low, which facilitates an increase in the Drude weight with electron temperature.

With this background, we now consider the observed temporal dynamics of the THz response of the photoexcited graphene and its dependence on laser fluence, as summarized in Figure 2. Figure 2a plots the increase in the THz waveform induced by the pump beam, measured at the maximum of the time domain waveform, as a function of the delay time. Neglecting the change in the spectral characteristics, this can be considered as yielding the temporal evolution of the decrease in the graphene conductivity. The sharp rise in the response corresponds to heating of the electrons by the pump pulse, resulting, as discussed above, in an enhanced scattering rate and decrease of conductivity. The relaxation to a value close to the initial response occurs as electronic system cools down by phonon emission. This time scale has been previously been identified to be in the range of 1−2 ps for roughly comparable excitation conditions.[68] The present study shows that photo-induced switching of graphene on the time scale of 1 ps can be readily achieved.

The fluence dependence of the graphene photoresponse is also interesting. The most pronounced effect is the strongly sublinear increase in the change of conductivity with pump fluence. This is apparent from the traces of Figure 2a and is plotted explicitly in Figure 2b. In this context, we note the Drude weight is a nonlinear function of the electronic temperature.[69] At relatively high pump fluence, the increase of the Drude weight will become more and more important. This will give rise to an increase in the graphene conductivity, which would compensate the decrease in the conductivity caused by an increased electron scattering rate. The balance of these factors provides a natural explanation for the apparent saturation behavior in the photoresponse with increasing pump fluence (Figure 2b). In addition to this factor related to the amplitude of the response, there is a modest increase in the decay time, which has been observed with increasing fluence (inset of Figure 2a). The reduced sensitivity of the response of the conductivity to the electronic temperature at high fluences can explain this trend, since the initial rise in the THz response will then be diminished and the apparent decay time lengthened. In the region of lower fluences, we observe a THz signal that scales as fluence, $F^{1/2}$ (Figure 2b). A similar relation was recently reported for the photocurrent generated in a graphene *pn* junction by femtosecond laser excitation.[72] This latter result was explained in terms of a supercollision cooling model for the electrons and a peak electronic temperature scaling as $F^{1/2}$ (based on the electron heat capacity). In the context of our THz measurement, the observed scaling with fluence would then suggest pump-induced increase in scattering rate, $\Delta\Gamma$, that varies as $F^{1/2}$ or, within the context of the interpretation of ref 72, with the peak transient electronic temperature.

In conclusion, high-quality CVD-grown single-layer graphene shows a clear signature of Drude-like conductance behavior at THz frequencies. Under excitation by a femtosecond optical pulse, we observe enhanced THz transmission response, corresponding to a pump-induced decrease in the graphene conductivity. The transient response relaxes on a time scale of 1−2 ps. We can explain both the sign of the photoinduced THz response and its spectral characteristics by electron heating. In our doped high mobility samples, the primary effect of electron heating is to increase the carrier scattering rate, without increasing the effective carrier concentration (or, more specifically, Drude weight) significantly. The different character of the photoinduced response reported here compared with previous studies highlights the variety of response possible in graphene depending on the sample mobility, doping, and excitation conditions.

AUTHOR INFORMATION

Corresponding Author

*E-mail: tony.heinz@columbia.edu.

Notes

The authors declare no competing financial interest.

■ ACKNOWLEDGMENTS

The authors acknowledge valuable discussions with Drs. Davide Boschetto, Nuh Gedik, Kin Fai Mak, and Jie Shan. This work was supported by the National Science Foundation (grant DMR-1106225) and through the MURI program of the Air Force Office of Scientific Research. G.J. gratefully acknowledges support from the Alexander-von-Humboldt foundation through a Feodor-Lynen Fellowship.

■ REFERENCES

(1) Novoselov, K. S.; Geim, A. K.; Morozov, S. V.; Jiang, D.; Katsnelson, M. I.; Grigorieva, I. V.; Dubonos, S. V.; Firsov, A. A. *Nature* **2005**, *438*, 197.
(2) Zhang, Y. B.; Tan, Y. W.; Stormer, H. L.; Kim, P. *Nature* **2005**, *438*, 201.
(3) Geim, A. K.; Novoselov, K. S. *Nat. Mater.* **2007**, *6*, 183.
(4) Morozov, S. V.; Novoselov, K. S.; Katsnelson, M. I.; Schedin, F.; Elias, D. C.; Jaszczak, J. A.; Geim, A. K. *Phys. Rev. Lett.* **2008**, *100*, 016602.
(5) Bolotin, K. I.; Sikes, K. J.; Jiang, Z.; Klima, M.; Fudenberg, G.; Hone, J.; Kim, P.; Stormer, H. L. *Solid State Commun.* **2008**, *146*, 351.
(6) Bonaccorso, F.; Sun, Z.; Hasan, T.; Ferrari, A. C. *Nat. Photonics* **2010**, *4*, 611.
(7) Avouris, P. *Nano Lett.* **2010**, *10*, 4285.
(8) Mak, K. F.; Sfeir, M. Y.; Wu, Y.; Lui, C. H.; Misewich, J. A.; Heinz, T. F. *Phys. Rev. Lett.* **2008**, *101*, 196405.
(9) Nair, R. R.; Blake, P.; Grigorenko, A. N.; Novoselov, K. S.; Booth, T. J.; Stauber, T.; Peres, N. M. R.; Geim, A. K. *Science* **2008**, *320*, 1308.
(10) Dawlaty, J. M.; Shivaraman, S.; Strait, J.; George, P.; Chandrashekhar, M.; Rana, F.; Spencer, M. G.; Veksler, D.; Chen, Y. *Appl. Phys. Lett.* **2008**, *93*, 131905.
(11) Yan, H. G.; Xia, F. N.; Zhu, W. J.; Freitag, M.; Dimitrakopoulos, C.; Bol, A. A.; Tulevski, G.; Avouris, P. *ACS Nano* **2011**, *5*, 9854.
(12) Wang, F.; Zhang, Y.; Tian, C.; Girit, C.; Zettl, A.; Crommie, M.; Shen, Y. R. *Science* **2008**, *320*, 206.
(13) Li, Z. Q.; Henriksen, E. A.; Jiang, Z.; Hao, Z.; Martin, M. C.; Kim, P.; Stormer, H. L.; Basov, D. N. *Nat. Phys.* **2008**, *4*, 532.
(14) Lemme, M. C.; Echtermeyer, T. J.; Baus, M.; Kurz, H. *IEEE Electron Device Lett.* **2007**, *28*, 282.
(15) Jablan, M.; Buljan, H.; Soljačić, M. *Phys. Rev. B* **2009**, *80*, 245435.
(16) Lin, Y. M.; Dimitrakopoulos, C.; Jenkins, K. A.; Farmer, D. B.; Chiu, H. Y.; Grill, A.; Avouris, P. *Science* **2010**, *327*, 662.
(17) Ju, L.; Geng, B.; Horng, J.; Girit, C.; Martin, M.; Hao, Z.; Bechtel, H. A.; Liang, X.; Zettl, A.; Shen, Y. R.; Wang, F. *Nat. Nanotechnol.* **2011**, *6*, 630.
(18) Liao, L.; Lin, Y.-C.; Bao, M.; Cheng, R.; Bai, J.; Liu, Y.; Qu, Y.; Wang, K. L.; Huang, Y.; Duan, X. *Nature* **2010**, *467* (7313), 305−308.
(19) Bao, Q.; Loh, K. P. *ACS Nano* **2012**, *6* (5), 3677−3694.
(20) Ando, T.; Zheng, Y. S.; Suzuura, H. *J. Phys. Soc. Jpn.* **2002**, *71*, 1318.
(21) Kuzmenko, A. B.; van Heumen, E.; Carbone, F.; van der Marel, D. *Phys. Rev. Lett.* **2008**, *100*, 117401.
(22) Horng, J.; Chen, C.-F.; Geng, B.; Girit, C.; Zhang, Y.; Hao, Z.; Bechtel, H. A.; Martin, M.; Zettl, A.; Crommie, M. F.; Shen, Y. R.; Wang, F. *Phys. Rev. B* **2011**, *83*, 165113.
(23) Tomaino, J. L.; Jameson, A. D.; Kevek, J. W.; Paul, M. J.; van der Zande, A. M.; Barton, R. A.; McEuen, P. L.; Minot, E. D.; Lee, Y.-S. *Opt. Express* **2011**, *19*, 141.
(24) Liu, W.; Aguilar, R. V.; Hao, Y. F.; Ruoff, R. S.; Armitage, N. P. *J. Appl. Phys.* **2011**, *110*, 083510.
(25) Sensale-Rodriguez, B.; Yan, R.; Kelly, M. M.; Fang, T.; Tahy, K.; Hwang, W. S.; Jena, D.; Liu, L.; Xing, H. G. *Nat. Commun.* **2012**, *3*, 780.
(26) Ren, L.; Zhang, Q.; Yao, J.; Sun, Z. Z.; Kaneko, R.; Yan, Z.; Nanot, S.; Jin, Z.; Kawayama, I.; Tonouchi, M.; Tour, J. M.; Kono, J. *Nano Lett.* **2012**, *12*, 3711.
(27) Maeng, I.; Lim, S.; Chae, S. J.; Lee, Y. H.; Choi, H.; Son, J. H. *Nano Lett.* **2012**, *12*, 551.
(28) Yan, H.; Li, Z.; Li, X.; Zhu, W.; Avouris, P.; Xia, F. *Nano Lett.* **2012**, *12*, 3766.
(29) Fei, Z.; Rodin, A. S.; Andreev, G. O.; Bao, W.; McLeod, A. S.; Wagner, M.; Zhang, L. M.; Zhao, Z.; Thiemens, M.; Dominguez, G.; Fogler, M. M.; Neto, A. H. C.; Lau, C. N.; Keilmann, F.; Basov, D. N. *Nature* **2012**, *487*, 82.
(30) Fei, Z.; Andreev, G. O.; Bao, W.; Zhang, L. M.; McLeod, A. S.; Wang, C.; Stewart, M. K.; Zhao, Z.; Dominguez, G.; Thiemens, M.; Fogler, M. M.; Tauber, M. J.; Castro-Neto, A. H.; Lau, C. N.; Keilmann, F.; Basov, D. N. *Nano Lett.* **2011**, *11*, 4701.
(31) Kampfrath, T.; Perfetti, L.; Schapper, F.; Frischkorn, C.; Wolf, M. *Phys. Rev. Lett.* **2005**, *95*, 187403.
(32) Sun, D.; Wu, Z.-K.; Divin, C.; Li, X.; Berger, C.; de Heer, W. A.; First, P. N.; Norris, T. B. *Phys. Rev. Lett.* **2008**, *101*, 157402.
(33) Dawlaty, J. M.; Shivaraman, S.; Chandrashekhar, M.; Rana, F.; Spencer, M. G. *Appl. Phys. Lett.* **2008**, *92*, 042116.
(34) Breusing, M.; Ropers, C.; Elsaesser, T. *Phys. Rev. Lett.* **2009**, *102*, 086809.
(35) Newson, R. W.; Dean, J.; Schmidt, B.; van Driel, H. M. *Opt. Express* **2009**, *17*, 2326.
(36) Wang, H.; Strait, J. H.; George, P. A.; Shivaraman, S.; Shields, V. B.; Chandrashekhar, M.; Hwang, J.; Rana, F.; Spencer, M. G.; Ruiz-Vargas, C. S.; Park, J. *Appl. Phys. Lett.* **2010**, *96*, 081917.
(37) Winnerl, S.; Orlita, M.; Plochocka, P.; Kossacki, P.; Potemski, M.; Winzer, T.; Malic, E.; Knorr, A.; Sprinkle, M.; Berger, C.; de Heer, W. A.; Schneider, H.; Helm, M. *Phys. Rev. Lett.* **2011**, *107*, 237401.
(38) George, P. A.; Strait, J.; Dawlaty, J.; Shivaraman, S.; Chandrashekhar, M.; Rana, F.; Spencer, M. G. *Nano Lett.* **2008**, *8*, 4248.
(39) Choi, H.; Borondics, F.; Siegel, D. A.; Zhou, S. Y.; Martin, M. C.; Lanzara, A.; Kaindl, R. A. *Appl. Phys. Lett.* **2009**, *94*, 172102.
(40) Strait, J. H.; Wang, H. N.; Shivaraman, S.; Shields, V.; Spencer, M.; Rana, F. *Nano Lett.* **2011**, *11*, 4902.
(41) Lee, E. J. H.; Balasubramanian, K.; Weitz, R. T.; Burghard, M.; Kern, K. *Nat. Nanotechnol.* **2008**, *3*, 486.
(42) Park, J.; Ahn, Y. H.; Ruiz-Vargas, C. *Nano Lett.* **2009**, *9*, 1742.
(43) Xu, X. D.; Gabor, N. M.; Alden, J. S.; van der Zande, A. M.; McEuen, P. L. *Nano Lett.* **2010**, *10*, 562.
(44) Lemme, M. C.; Koppens, F. H. L.; Falk, A. L.; Rudner, M. S.; Park, H.; Levitov, L. S.; Marcus, C. M. *Nano Lett.* **2011**, *11*, 4134.
(45) Gabor, N. M.; Song, J. C. W.; Ma, Q.; Nair, N. L.; Taychatanapat, T.; Watanabe, K.; Taniguchi, T.; Levitov, L. S.; Jarillo-Herrero, P. *Science* **2011**, *334*, 648.
(46) Song, J. C. W.; Rudner, M. S.; Marcus, C. M.; Levitov, L. S. *Nano Lett.* **2011**, *11*, 4688.
(47) Sun, D.; Aivazian, G.; Jones, A. M.; Ross, J. S.; Yao, W.; Cobden, D.; Xu, X. *Nat. Nanotechnol.* **2012**, *7*, 114.
(48) Prechtel, L.; Song, L.; Schuh, D.; Ajayan, P.; Wegscheider, W.; Holleitner, A. W. *Nat. Commun.* **2012**, *3*, 646.
(49) Nazin, G.; Zhang, Y.; Zhang, L.; Sutter, E.; Sutter, P. *Nat. Phys.* **2010**, *6*, 870.
(50) Xia, F.; Mueller, T.; Lin, Y.-m.; Valdes-Garcia, A.; Avouris, P. *Nat. Nanotechnol.* **2009**, *4*, 839.
(51) Mueller, T.; Xia, F. N. A.; Avouris, P. *Nat. Photonics* **2010**, *4*, 297.
(52) Li, X. S.; Cai, W. W.; An, J. H.; Kim, S.; Nah, J.; Yang, D. X.; Piner, R.; Velamakanni, A.; Jung, I.; Tutuc, E.; Banerjee, S. K.; Colombo, L.; Ruoff, R. S. *Science* **2009**, *324*, 1312.
(53) Nahata, A.; Auston, D. H.; Heinz, T. F.; Wu, C. J. *Appl. Phys. Lett.* **1996**, *68*, 150.
(54) Wu, Q.; Zhang, X. C. *Appl. Phys. Lett.* **1995**, *67*, 3523.
(55) Nahata, A.; Weling, A. S.; Heinz, T. F. *Appl. Phys. Lett.* **1996**, *69*, 2321.
(56) Tinkham, M. *Phys. Rev. B* **1956**, *104*, 845.
(57) Hegmann, F. A.; Ostroverkhova, O.; Cooke, D. G. *Photophysics of Molecular Materials*; Wiley-VCH: Weinheim, 2006; p 367.

(58) Parker, T. J.; Ford, J. E.; Chambers, W. G. *Infrared Phys.* **1978**, *18*, 215.
(59) Naftaly, M.; Miles, R. E. *Proc. IEEE* **2007**, *95*, 1658.
(60) Buron, J. D.; Petersen, D. H.; Bøggild, P.; Cooke, D. G.; Hilke, M.; Sun, J.; Whiteway, E.; Nielsen, P. F.; Hansen, O.; Yurgens, A.; Jepsen, P. U. *Nano Lett.* **2012**, *12*, 5074.
(61) Hwang, E. H.; Adam, S.; Das Sarma, S. *Phys. Rev. Lett.* **2007**, *98*, 186806.
(62) Nomura, K.; MacDonald, A. H. *Phys. Rev. Lett.* **2007**, *98*, 076602.
(63) Peres, N. M. R.; Lopes dos Santos, J. M. B.; Stauber, T. *Phys. Rev. B* **2007**, *76*, 073412.
(64) Castro Neto, A. H.; Guinea, F.; Peres, N. M. R.; Novoselov, K. S.; Geim, A. K. *Rev. Mod. Phys.* **2009**, *81*, 109.
(65) Ando, T. *J. Phys. Soc. Jpn.* **2006**, *75*, 074716.
(66) Nienhuys, H.-K.; Sundström, V. *Phys. Rev. B* **2005**, *71*, 235110.
(67) Knoesel, E.; Bonn, M.; Shan, J.; Wang, F.; Heinz, T. F. *J. Chem. Phys.* **2004**, *121*, 394.
(68) Lui, C. H.; Mak, K. F.; Shan, J.; Heinz, T. F. *Phys. Rev. Lett.* **2010**, *105*, 127404.
(69) Gusynin, V. P.; Sharapov, S. G.; Carbotte, J. P. *New J. Phys.* **2009**, *11*, 095013.
(70) Yan, H. G.; Song, D. H.; Mak, K. F.; Chatzakis, I.; Maultzsch, J.; Heinz, T. F. *Phys. Rev. B* **2009**, *80*, 121403.
(71) Chen, J.-H.; Jang, C.; Xiao, S.; Ishigami, M.; Fuhrer, M. S. *Nat. Nanotechnol.* **2008**, *3*, 206.
(72) Graham, M. W.; Shi, S.-F.; Ralph, D. C.; Park, J.; McEuen, P. L. *Nat. Phys.* 2012, advance online publication; DOI: 10.1038/nphys2493.